A Study on the Radiation Hardness of Lead Tungstate Crystals [1]

R.Y. Zhu[2], Q. Deng[3], H. Newman[2], C.L. Woody[4], J.A. Kierstead[4] and S.P. Stoll[4]

[2]256-48, HEP, California Institute of Technology, Pasadena, CA 91125

[3]Shanghai Institute of Ceramics, Chinese Academy of Sciences, Shanghai 200050

[4]Physics Department, Brookhaven National Laboratory, Upton, NY 11973

Abstract

This report presents recent progress of a study on the radiation damage in lead tungstate ($PbWO_4$) crystals. The dose rate dependence of radiation damage in $PbWO_4$ has been observed. An optimization of the oxygen compensation through post-growth thermal annealing has led to $PbWO_4$ samples with significantly improved radiation hardness. Front irradiation is found to cause a factor of 2 to 6 times less severe damage than uniform irradiation. Lanthanum doping was found not to be a determining factor for $PbWO_4$ radiation hardness improvement. Finally, a TEM/EDS analysis revealed that the radiation damage in $PbWO_4$ crystals is caused by oxygen vacancies.

I. INTRODUCTION

Because of its high density and fast decay time, lead tungstate ($PbWO_4$) crystals were chosen by the CMS experiment to construct a precision electromagnetic calorimeter at LHC [1]. Our previous studies on $PbWO_4$ samples revealed that $PbWO_4$ crystals suffer from non-negligible radiation damage after a dose as low as 10 rad [2], but the scintillation mechanism of $PbWO_4$ is not affected by the radiation, i.e. the loss of light output is due only to absorption by radiation induced color centers [3]. We also proposed that the damage in $PbWO_4$ is caused by structure related defects, such as oxygen vacancies [2], and the level of the damage may be dose rate dependent because of the damage recovery observed [4].

In this report, we present progress in our understanding on the radiation damage in $PbWO_4$ crystals. Section II describes a dose rate dependence and the result of an optimization of the oxygen compensation, carried out at Shanghai Institute of Ceramics (SIC). A comparison of different irradiation patterns is presented in Section III. Section IV discusses the results of measurements of a preliminary batch of lanthanum (La) doped $PbWO_4$ samples. A microscopic analysis using Transmission Electron Microscopy (TEM) coupled to Energy Dispersion Spectrometry (EDS) is presented in Section V. This work is a part of an ongoing effort aimed at developing radiation hard $PbWO_4$ crystals for CMS at LHC [5].

II. DOSE RATE DEPENDENCE AND OPTIMIZATION OF OXYGEN COMPENSATION

Twelve $PbWO_4$ samples were measured to study the effect of post-growth oxygen compensation on the radiation hardness of $PbWO_4$ crystals. Table 1 lists their dimensions, date of delivery and the conditions used for post-growth thermal annealing.

Table 1
PbWO$_4$ Samples Tested for Oxygen Compensation

ID	Dimension (cm)	Date	Annealing
BGRI 1	$2.3 \times 5 \times 2.3$	1/97	-
SIC 93	$2.5 \times 5 \times 2.5$	1/97	-
SIC 115-1	$2 \times 5 \times 2$	1/97	O_2-1
SIC 121-1	$2 \times 5 \times 2$	1/97	O_2-1
SIC 117-1	$2 \times 5 \times 2$	1/97	O_2-2
SIC 122-1	$2 \times 5 \times 2$	1/97	O_2-2
SIC 115-2	$2 \times 5 \times 2$	1/97	Air-1
SIC 121-2	$2 \times 5 \times 2$	1/97	Air-1
SIC 116-2	$2 \times 5 \times 2$	1/97	Air-2
SIC 117-2	$2 \times 5 \times 2$	1/97	Air-2
SIC 152-2	$2 \times 5 \times 2$	8/97	Optimized O_2
SIC 153	$2 \times 5 \times 2$	8/97	Optimized O_2

Samples were prepared in 6 different annealing conditions, ranging from no annealing at all, two kinds of annealing in air: Air-1 and Air-2, and three kinds of annealing in oxygen: O_2-1, O_2-2 and final optimized O_2. The difference between different annealing conditions is in the temperature, duration and partial pressure of the oxygen in the oven. In order to test the reproducibility of the procedure, each annealing condition was tested using a pair of crystals cut from different boles. In addition, two samples from the same bole were treated with different annealing conditions (e.g., 115-1 and 115-2 were treated in oxygen and air, respectively). All samples, except BGRI 1, were grown at SIC.

Samples were wrapped with aluminum foil, and were placed at a fixed distance to a γ-ray source to receive a defined dose rate. Samples were under irradiation all the time, except when measurements were carried out, which typically lasted for about 20 minutes. The absolute light output was measured using a Hamamatsu R2059 PMT with a small ^{137}Cs source placed at the far end of the crystal. The systematic uncertainty of the light output due to temperature variation in the lab is less than 0.3%. The overall systematic uncertainty of the light

III. FRONT VERSUS UNIFORM IRRADIATIONS

Two most common irradiation patterns are uniform and front irradiations. In front irradiation, the radiation is applied perpendicular to the small end of a long sample. In uniform irradiation, the radiation is applied perpendicular to one long side of the crystal, and uniformity along the length. With a γ-ray irradiation source, the uniform irradiation exposes the entire volume of the crystal, while the front irradiation only exposes a few centimeters at the front.

Table 2
Samples Tested for Front and Uniform Irradiations

ID	Dimension (cm)	Date	Annealing
SIC 85	$2.0 \times 20 \times 2.3$	8/96	O_2
SIC 135	$2.0 \times 23 \times 2.3$	5/97	O_2
SIC 136	$2.0 \times 23 \times 2.3$	5/97	O_2

A total of three full size samples were tested, as shown in Table 2. These samples have a tapered shape with small and large ends of 2 and 2.3 cm square respectively, and a length of 20 to 23 cm. Samples were prepared through our standard process of thermal annealing at 250°C for two hours and were irradiated at a fixed dose rate of 15, 100 and 480 rad/h. At each dose rate, the light output of these samples were measured until they reached equilibrium, as defined by no change of light output in 24 hours under irradiation. After that, the dose rate was increased to the next higher level. The same procedure was followed for both front and uniform irradiations. We found that the light output degradation under uniform irradiation is a factor of 2 to 6 worse than that of front irradiation. A typical result is shown in Figure 4 for sample 85. While this sample suffered a damage of 2% at 15 rad/h under front irradiation,

it was increased to about 8% under uniform irradiation. The uniform irradiation caused much more severe damage, since color centers were created in the entire body of the crystal.

IV. EFFECT OF LANTHANUM DOPING

The doping of lanthanum in $PbWO_4$ crystals is known to improve the UV cut-off edge of the transmittance [6]. In the process of developing rad-hard $PbWO_4$ crystals for CMS, we also recognized that lanthanum doping might be an alternative approach to reduce the density of oxygen vacancies. Lanthanum doping is carried out by introducing La_2O_3 powder in raw material. This results in one molecule of La_2O_3 replacing two PbO molecules and, consequently, filling one oxygen vacancy. A preliminary batch of lanthanum doped samples were grown at SIC to test the effectiveness of La doping. Table 3 lists the sample ID, dimension, annealing condition and the amount of lanthanum in the raw material. All samples were delivered in June, 1997.

Table 3
Samples Tested for the La Doping

ID	Dimension (cm)	Annealing	La (ppm)
SIC L-1	$2 \times 5 \times 2$	O_2	1960
SIC L-5	$2 \times 5 \times 2$	-	168
SIC L-6	$2 \times 5 \times 2$	-	84

We found that La doping indeed improves the UV cut-off edge of the transmission, confirming the earlier observation by Kobayashi et al. [6]. Figure 5 shows the longitudinal transmission of sample SIC L-5 , measured with a Hitachi U-3210 spectrophotometer before irradiation and

Fig. 4 Light output degradation at equilibrium is shown as a function of dose rate for uniform and front irradiations for sample SIC 85.
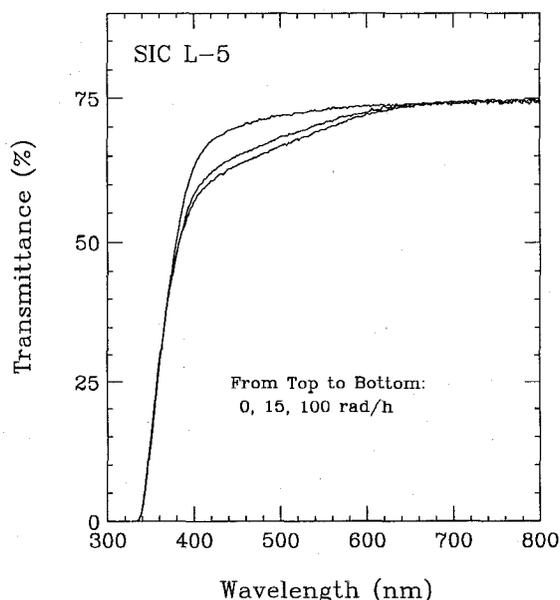
Fig. 5 Transmittance at equilibrium at different dose rates is shown as a function of wavelength for sample SIC L-5.
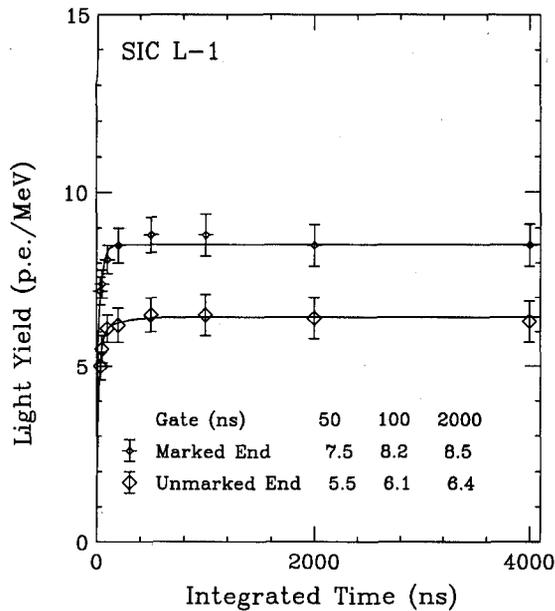
Fig. 6 Light output of sample SIC L-1 is plotted as a function of integration time, showing different amplitudes when different ends of the sample were coupled to the PMT.

Fig. 7 Normalized light output at equilibrium is shown as a function of dose rate for three La doped samples, and compared to oxygen annealed sample SIC 153.

at equilibrium at dose rates of 15 and 100 rad/h. A very sharp rising at 340 nm was observed both before and after irradiation, as compared to samples without La doping. A radiation-induced absorption band peaked at 420 nm, however, is clearly observed for this sample. The transmittance of the other La doped samples show similar features, indicating that La doping alone does not improve the radiation hardness.

We also found that the peak of the emission spectrum of La doped samples shifted from the green (500 nm) to the blue (420 nm), and the light output of these samples is sensitive to the La concentration, indicating that La doping may change the PbWO$_4$ scintillation mechanism. To verify this, the light output was measured as a function of integration time for each sample with two different ends coupled to the PMT. Figure 6 shows the result for sample SIC L-1. While the light output of La doped samples is indeed faster than samples without La doping, it depends on the end coupled to the PMT. Thirty percent more light was observed for sample SIC L-1 after switching the end coupled to the PMT. This highly non-uniform light output was observed in all three La doped samples, but was not observed in any undoped sample.

Assuming La doping affects the PbWO$_4$ scintillation, this non-uniformity may be caused by a non-uniform La concentration in the sample. A Glow Discharge Mass Spectroscopy (GDMS) analysis was carried out at Shiva Technologies West, Inc., California. Table 4 shows the result of the trace element analysis, in ppm by weight, for five pieces of PbWO$_4$ samples: three pieces from the top, middle and bottom portion of sample SIC L6, and two pieces from two ends of another sample L4. As seen from this table, the La concentration is indeed not uniform within the sample. We thus conclude that the origin of this light output non-uniformity is due to very different La concentrations in the sample caused by
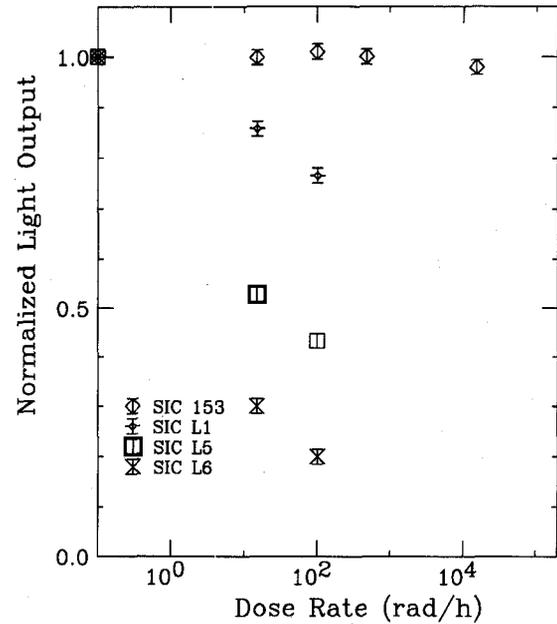
a segregation coefficient not equal to one. Table 4 also indicates that while impurities of Na, K, Mo, As and Eu moved to the top of the crystal during the growth process with a segregation coefficient of less than one, impurities of Ca and La stayed at the bottom of the crystal with a segregation coefficient larger than one. Note that SIC uses a modified Bridgman method to grow PbWO$_4$ crystals from the bottom up.

Finally, it is concluded that La doping alone does not improve PbWO$_4$ radiation hardness. Figure 7 shows the normalized light output at equilibrium under specific dose rates for these La doped samples, and compared to sample 153 which is treated with optimized oxygen compensation. It is clear that SIC 153 has much better radiation hardness than all of the La doped samples. Note, however, this batch of La doped samples was preliminary, and further efforts will be made to dope lanthanum more uniformly in PbWO$_4$. As discussed above, La doping indeed improves the transmittance of the crystal, and may help in reducing oxygen vacancies. Therefore, La and other tri-valent doping studies will continue until a final conclusion is drawn.

V. LEAD TUNGSTATE DAMAGE MECHANISM

Crystal defects, such as oxygen vacancy, are known to cause radiation damage for other oxide scintillators. In BGO, for example, three common radiation induced absorption bands at 2.3, 3.0 and 3.8 eV with consistent widths were found in a series of 24 doped samples [7], indicating defect-related color centers.

In our previous work, we concluded that PbWO$_4$ damage is caused by structure related defects, such as oxygen vacancies [2]. This conclusion was reached based upon material analysis carried out for a batch of PbWO$_4$ crystals grown in Bogoroditsk Techno-Chemical Plant (BTCP), Russia, and SIC. We first did GDMS analysis at Charles Evens & Associates, California.

Table 4
Trace Impurity Result (ppmw) Obtained by GDMS Analysis for Five La Doped $PbWO_4$ Samples

ID	Na	Al	Si	K	Ca	La	Mo	As	TE	Eu
L-6 (T)	9.1	0.2	0.3	1.4	0.8	2.7	1.3	0.93	0.2	4.3
L-6 (M)	2.7	0.04	0.4	0.7	2.9	38	0.92	0.19	0.01	2.1
L-6 (B)	1.9	0.1	0.2	0.5	6.2	85	0.84	0.13	0.02	1.5
L-4 (T)	1.4	0.4	0.5	5.9	0.05	2.8	1.8	3.9	0.2	1.2
L-4 (B)	0.2	0.7	0.6	0.4	0.38	590	0.68	0.64	0.1	0.6

A survey of 76 elements, including all of the lanthanides, indicates that there are no obvious correlations between the detected trace impurities and the crystal's susceptibility to radiation damage. This indicates an important role of defects, such as oxygen vacancies, which cannot be determined by GDMS. We then did Particle Induced X-ray Emission (PIXE) and quantitative wavelength dispersive Electron Micro-Probe Analysis (EMPA) at Charles Evans & Associates, and found that crystals with poor radiation hardness had an abnormal stoichiometric W/Pb ratio.

As discussed in Section II, we have observed a significant improvement in the radiation hardness of $PbWO_4$ crystals from oxygen compensation through post-growth thermal annealing in an oxygen-rich atmosphere. This is a pragmatic approach to develop radiation hard $PbWO_4$ crystals, but is not a direct observation of oxygen vacancies in the crystal. To directly observe oxygen vacancies, one must be able to measure the complete stoichiometric ratio of Pb:W:O in $PbWO_4$ samples. Efforts have been made along this line. X-ray Photoelectron Spectroscopy (XPS) was tried at Charles Evens & Associates [8]. However, it was found to be very difficult due to the systematic uncertainty in the oxygen analysis. Effort has also be made to directly identify oxygen vacancies by Electron Paramagnetic Resonance (ESR) and Electron-Nuclear Double Resonance (ENDOR) through observing unpaired electrons. However, it too was also difficult to reach a quantitative conclusion.

By using Transmission Electron Microscopy (TEM) coupled to Energy Dispersion Spectrometry (EDS), a localized stoichiometry analysis was possible to identify oxygen vacancies. A TOPCON-002B Scope was first used at 200 kV and 10 μA. Samples were made into powders of an average grain size of a few μm, and then placed on a sustaining
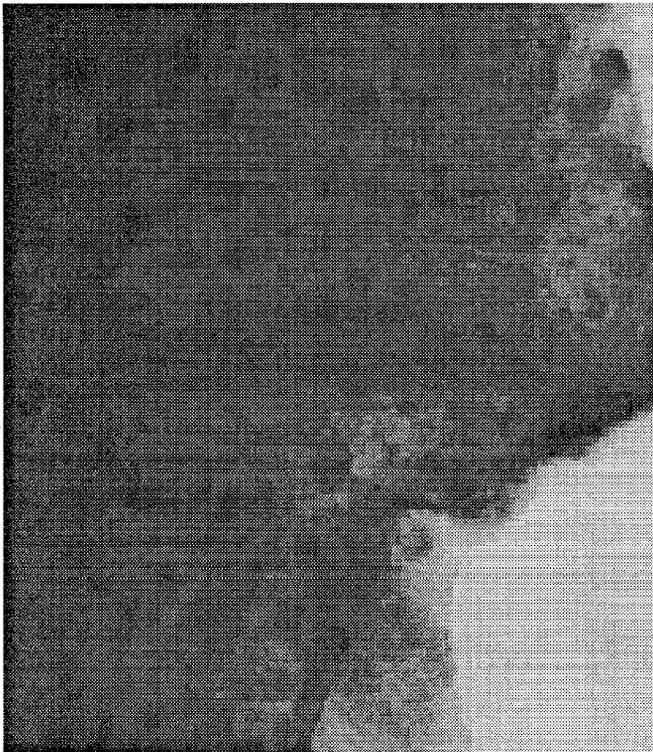
Fig. 8 TEM picture of a $PbWO_4$ sample with poor radiation hardness, showing black spots of ϕ5–10 nm related to oxygen vacancies.
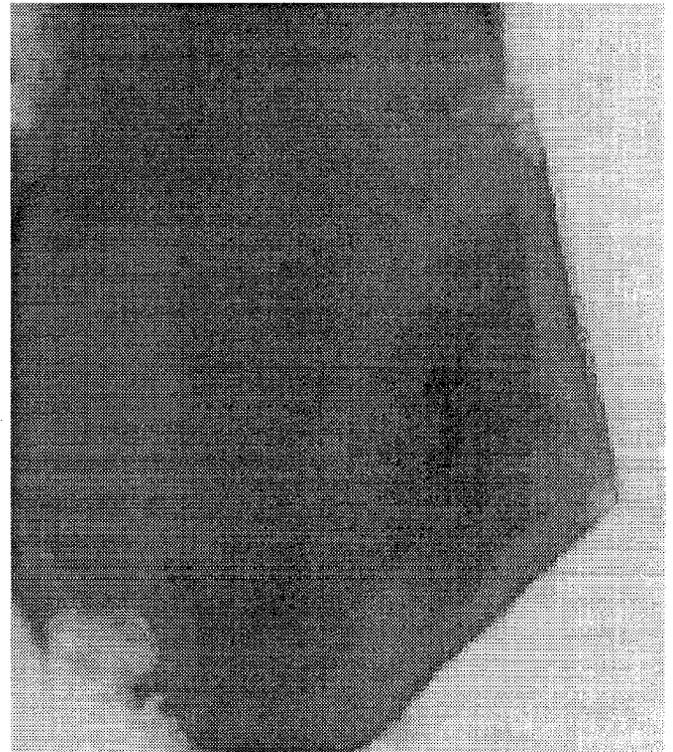
Fig. 9 TEM picture of a $PbWO_4$ crystal with good radiation hardness, showing no black spots.

membrane. With a spatial resolution of 2 Å, the lattice structure of $PbWO_4$ crystals was clearly visible.

Figure 8 shows a TEM picture taken for a sample with poor radiation hardness. Some black spots of a diameter of 5 – 10 nm are clearly seen in the picture. On the other hand, samples with good radiation hardness show a stable TEM picture with no black spots (Figure 9).

By employing TEM with an EDS system, a localized stoichiometry analysis was carried out at SIC. The system is a JEOL JEM-2010 scope and a Link ISIS EDS. The spatial resolution of this system allows a localized stoichiometry analysis in a region with a diameter of 0.5 nm [9]. An as grown sample was first analyzed, and black spots were observed. Points inside and surrounding the black spots were analyzed as well as points far away from the black spots. The uncertainty of the analysis is typically 15%. The result of this analysis is listed in Table 5, where atomic fractions (%) in these areas are shown. The results show a deviation from the atomic stoichiometry of O:W:Pb = 66:17:17 in the center of the black spots, pointing to a severe deficit of the oxygen component. In the peripheral area, the oxygen deficit is less, but still significant. There is no oxygen deficit observed in the area far away from the black spots. This analysis thus positively identified oxygen vacancies in $PbWO_4$.

Table 5
Atomic Fraction (%) of $PbWO_4$ Obtained with Localized ($\phi 0.5$ nm) Stoichiometry Analysis by TEM/EDS

As Grown Sample

Element	Black Spot	Peripheral	Matrix$_1$	Matrix$_2$
O	1.5	15.8	60.8	63.2
W	50.8	44.3	19.6	18.4
Pb	47.7	39.9	19.6	18.4

The Same Sample after Oxygen Compensation

Element	Point$_1$	Point$_2$	Point$_3$	Point$_4$
O	59.0	66.4	57.4	66.7
W	21.0	16.5	21.3	16.8
Pb	20.0	17.1	21.3	16.5

As a comparison, the same sample after oxygen compensation was re-analyzed. No black spots were found. The result of the analysis is also listed in Table 5. In all randomly selected points, no stoichiometry deviations were observed. This analysis thus clearly identified oxygen vacancies in $PbWO_4$ samples of poor radiation hardness, and confirmed our early conjecture on the $PbWO_4$ radiation damage mechanism.

VI. SUMMARY

A brief summary of the investigation carried out in this report is listed below.

1. The level of radiation damage in $PbWO_4$ crystals is dose rate dependent — a confirmation of *our prediction* published in reference [4].

2. The oxygen compensation through post-growth thermal annealing is effective in improving $PbWO_4$ radiation hardness, and has led to 5 cm $PbWO_4$ samples of significantly improved radiation hardness. The effect of annealing on the radiation hardness of $PbWO_4$ crystals is reproducible.

3. The light output degradation under uniform irradiation is a factor of 2 to 6 worse than that of front irradiation.

4. Investigation of a preliminary batch of La-doped samples indicates that La doping does improve the UV cut-off edge of the transmission and increases the fast component light output, but does not appear to improve the radiation hardness. The investigation of La doping will continue in order to reach a final conclusion.

5. The $PbWO_4$ damage mechanism is understood as being due to structure related defects, e.g. oxygen vacancies. These defects were clearly identified by a localized stoichiometry analysis using TEM/EDS. This also explains the effectiveness of oxygen compensation in improving the radiation hardness of $PbWO_4$ crystals

VII. ACKNOWLEDGMENTS

VIII. REFERENCES

[1] *Compact Muon Solenoid Technical Proposal*, CERN/LHCC 94-38, LHCC/P1 (1994).

[2] R.Y. Zhu *et al.*, *Nucl. Instr. and Meth.* A376 319 (1996); C. Woody *et al.*, in *Proceedings of SCINT95 Int'l Conf.* Delft, August 1995 and *IEEE-NUCL-S* V43 (1996) 1585.

[3] R.Y. Zhu *et al.*, in *Proc. of the 6th Int. Conf. on Calorimetry in High Energy Physics*, ed. A. Antonelli *et al.*, Frascati Physics Series (1996) 577.

[4] R.Y. Zhu, *IEEE Trans. Nucl. Sci.* NS-44 468 (1997).

[5] See chapter 2 of *CMS Electromagnetic Calorimeter Technical Design Report*, CERN/LHCC 97-33 and references therein, and papers from P. Lecoq, P. Lecomte and R.Y. Zhu in *Proc. of the 7th Int. Conf. on Calorimetry in High Energy Physics*, Tucson, November 1997.

[6] M. Kobayashi *et al.*, *Nucl. Instr. and Meth.* A399 261 (1997) and *KEK Preprint 97-12*.

[7] R.Y. Zhu *et al.*, *Nucl. Instr. and Meth.* A302 69 (1991),

[8] C. Lazik of Charles Evans and Associates, private communications.

[9] Z.W. Yin *et al.*, in *Proceedings of SCINT97 Int'l Conf.*, Shanghai, September 1997.